Lawrence Berkeley National Laboratory
Recent Work

Title
RECENT EXPERIMENTS ON FORMING ELECTRON RINGS AT BERKELEY

Permalink
https://escholarship.org/uc/item/1p92t7p5

Authors
Lambertson, G.R.
Keefe, D.
Laslett, L.J.
et al.

Publication Date
1971-02-01

UCRL-20183
Preprint

$C.2$

RECENT EXPERIMENTS ON
FORMING ELECTRON RINGS AT BERKELEY

G. R. Lambertson, D. Keefe, L. J. Laslett,
W. A. Perkins, J. M. Peterson and J. B. Rechen

February 1971

LAWRENCE RADIATION LABORATORY
UNIVERSITY of CALIFORNIA BERKELEY

UCRL-20183
$C.2$

DISCLAIMER

RECENT EXPERIMENTS ON FORMING ELECTRON RINGS AT BERKELEY[*]

G.R. Lambertson, D. Keefe, L.J. Laslett, W.A. Perkins,

J.M. Peterson and J.B. Rechen

Lawrence Radiation Laboratory
University of California
Berkeley, California

Summary

In the initial electron-ring experiments with a new high-current, 2 MeV electron injector an efficient method of trapping of the injected beam was developed, and a suitable compression cycle was found in which betatron amplitude growth on single-particle resonances is negligible. The ring behavior is satisfactory during the compression cycle at low intensity ($N_e < 5 \times 10^{11}$). At higher intensities the lowest mode of the coherent radial instability appeared, but the threshold for its onset was raised considerably by increasing the Landau damping coefficient, so that it is no longer the limiting instability. At intensities $N_e > 10^{12}$ electrons a longitudinal (negative mass) instability causes particle loss and radial spreading of the electron rings. Increasing the energy spread in the beam has raised the threshold for several phenomena observed in connection with this instability. The effects of changing the electromagnetic environment of the electron rings to suppress this instability are being investigated.

Introduction

Recent experiments in the Berkeley program[1] of electron-ring research have focused on the problems of ring instabilities. The importance of instabilities became evident in previous electron-ring experiments[2], in which comparatively small changes in the compressor resulted in severe losses in intensity and degradation in beam quality. Both collective phenomena and single-particle betatron resonances seemed to be involved.

The present electron-ring experiments were begun in September, 1970, when the first section (2 MeV energy) of the new, high-current (several hundred amperes) electron accelerator[3] was completed. In order to study the collective phenomena and the problem of crossing betatron resonances in the early part of a compression cycle, we assembled a relatively simple and flexible compressor system, in which the electromagnetic environment could be more easily understood and varied than in our previous systems. These experiments are still underway and will continue until we feel that we have enough understanding and control of these phenomena to proceed with confidence to the next step in the program -- experiments in the acceleration of ions.

Apparatus

A cross-sectional view of the apparatus (called Compressor 4) is shown in Fig. 1. In many respects it is similar to the Compressor 2 apparatus[4] in which rings containing $N_e = 4 \times 10^{12}$ electrons were successfully formed and compressed. The vacuum chamber is made of alumina and, the typical operating pressure (adequate for compression studies) is in the low 10^{-6} torr range. The compression Coil Sets 1 and 2 were initially located in the same positions as in Compressor 2 with provision for easy variation of their axial locations. Because we were interested only in the early stages of ring-formation and compression we decided to omit Coil Set 3, used for compression to small radius. Multiple-wedge foils can be inserted in the beam line to vary the instantaneous energy spread of the injected beam.

Simplified inflector electrodes that produce a pulsed field in the lower half of the chamber have been used for stacking either one or three turns of injected beam.

Diagnostics used included: A Rogowski coil around the injection snout to measure injected current; Faraday cups to monitor the injected electron trajectories by detecting the arrival of first and later turns; two collector probes, one movable in radius only, the other in both radius and azimuth; a variety of magnetic pickup loops to measure ring current and its high frequency modulation; scintillators to detect x-rays produced when the electrons strike the probes or other obstacles; and X-band and L-band detectors to record high frequency radiation in the 1-20 GH_z region.

Results

These experiments are still in progress; this report gives the current state of our knowledge and some tentative conclusions.

a) Betatron resonances

In previous compressor experiments we had found that a single-particle betatron resonance could be damaging or not, depending on the speed of crossing and the strength of the appropriate driving forces at that point. An important parameter is the so-called "n trajectory", which is the variation of the magnetic index $n \equiv - (R/B)(dB/dR)$ with radius during the compression cycle. For good operation this n trajectory should avoid crossing resonant values (n = 1/2, 4/9, ...) at radii where the driving terms are appreciable. Enlargement of the beam due to resonant growth at certain of these n values was observed during initial operation of Compressor 4, but a set of suitable n trajectories was arrived at through appropriate programming of currents in both coil sets. Generally most of the experimental results on collective effects were done using an n trajectory that stayed roughly constant near n = 0.45 for the first few centimeters of compression and then moved downward through n = 0.36.

Suitable choice of the magnitudes and time-dependences of the currents in the coils needed to achieve good n trajectories was arrived at not by empirical adjustment, but with the aid of a comprehensive computer program, NUERA[5]. While earlier forms date back some years, this program has in recent months reached a high degree of sophistication in simulating the effects of eddy currents (which often shift the n values by as much as 0.2) in the conductor material (9 mm square copper bar) used to make the coils. Measured values of fields and field gradients from various coil configurations were used in the development of the program to evaluate certain effective circuit parameters and to determine the degree of complexity needed to simulate eddy current effects.

A novel opportunity to test the accuracy of the

NUERA program arose when a transverse coherent instability was observed (see below). The frequency of this precessional mode is $(1 - \nu_R)f_0$, where f_0 is the gyrofrequency and ν_R is the radial betatron tune. This frequency was typically in the range 50 - 100 MHz, depending on the n trajectory chosen, and could be measured to a precision of 2%, or so. This allowed an experimental determination of n and it differed from the calculated value by only 0.02 which is within the accuracy of the measurement.

b) Transverse Coherent Instability

After satisfactory n trajectories had been achieved, it was observed that at a level of $N_e \approx 5 \times 10^{11}$, a strong transverse coherent radial instability occurred in the lowest mode, describable as a precessional motion of the ring as a whole with a frequency, $S = (1 - \nu_R)f_0$. This instability showed up quite clearly in oscillograms such as those in Figure 2. The traces on the left show the current collected on a probe placed at radius of 12 cm and the x-rays produced therefrom, and the picture on the right side shows a corresponding r-f burst picked up by a loop antenna. The multiple exposure shows that some rings were formed and later wiped off on the probe having undergone normal compression (late pulses) while others were completely wiped off at about 20 μsec after injection -- long before the equilibrium closed-orbit had been compressed to the radius of the probe. This can be understood in terms of a large coherent radial amplitude, and analysis of the corresponding r-f bursts associated with this behavior showed a dominant frequency, $(1 - \nu_R) f_0$. The multiple traces in Fig. 2 correspond to the same nominal injected beam intensity, and onset or not of the instability appeared to be determined by fluctuations from pulse to pulse, thus indicating a rather sharp threshold in intensity. This threshold was observed to move to higher values when the side plates were made of lower resistance as predicted from understanding of the resistive-wall driving term. As the intensity of the beam was increased above threshold, the onset of the instability and beam loss occurred earlier in time.

The threshold should be shifted to a higher value by an increase in the Landau damping that arises from the frequency spread

$$\Delta S = \frac{\partial S}{\partial E} \, \Delta E + \frac{\partial S}{\partial a^2} \, \Delta a^2$$

where E is the electron energy and "a" is the radial betatron amplitude. The coefficients of the differentials depend on n and $\frac{\partial n}{\partial r}$; the second term on the right hand side is rather small in Compressor 4. There were two puzzling features about the experimental observations. First, the threshold current and time of onset of the instability were found to be essentially unaffected by increasing the injected beam energy spread from $\Delta E/E < 0.5\%$ to $\Delta E/E \approx 2\%$. Second, there was the observation in the early Compressor 2 experiment[+] of ring currents an order of magnitude higher without any evidence of this instability, and yet the locations of Coil Sets 1 and 2 in the old and present compressors were the same.

The suggestion made by Sessler[6] that a zero in the coefficient $\frac{\partial S}{\partial E}$ could lead to a virtually undamped situation independent of ΔE proved to be correct. A careful examination of the structure and magnitude of the $\frac{\partial S}{\partial E}$ term showed[7] that indeed this coefficient came very close to zero about 20 μsec after injection

(Curve a, Fig. 3). The sharp drop in $\frac{\partial S}{\partial E}$ at that time was largely due to an unfriendly contribution to $\frac{\partial n}{\partial r}$ from eddy-currents in Coil Set 2. Further computation for the geometry of the coils in Compressor 2, led to a resolution of the second puzzle, illustrated by Curve c (Fig. 3) which shows that the $\frac{\partial S}{\partial E}$ term did not in that case come very close to zero. While Coil 2 there produced unfriendly contributions to $\frac{\partial n}{\partial r}$ because of eddy currents, these were nullified by eddy-current contributions favorable in sign due to the presence of Coil Set 3 in that experiment and absent in the current compressor!

Further computation for Compressor 4 showed that replacement of Coil Set 2 by stranded conductor (which would have negligible eddy-current effects) would lead to behavior of $\frac{\partial S}{\partial E}$ shown in Curve b (Fig. 3). When this physical change was made, the transverse instability became no longer limiting, presumably because the threshold had been shifted to a substantially higher value because of Landau damping. At how high a current level this instability will again cause trouble is not yet known.

c) Longitudinal Instability

Studies have been in progress for the past several weeks on a longitudinal instability which is presently limiting compact rings to an intensity $N_e \lesssim 10^{12}$. Phenomenologically the observations can be briefly summarized as follows. At low injected current levels ($\lesssim$ 30A), electrons trapped in the initial injection process continue to circulate without significant further losses; at higher injected currents, rapid and increasing losses are observed. Figure 4 shows the circulating beam current during the first 200 turns or so (time for 1 turn $\approx$ 4 nsec). A probe of the inner-radius envelope of the beam indicates rapid radial spreading of the beam accompanied by a decrease ($\geqslant$ 1 cm) in the mean closed orbit radius during the first few tens of turns at the highest current levels. Thus, the loss of beam shown in Fig. 4 probably corresponds to radial scraping of the beam on the injection-snout septum.

Magnetic pick-up loops with good high-frequency response allow one to observe the development of signals at the cyclotron-frequency (f_0) and a few higher harmonics (Fig. 5). At the lowest currents the r-f activity is small and, as the current is increased, one observes a developing growth (in tens of turns) of modulation at f_0, at higher current a more rapid growth at f_0 followed by the onset of higher harmonics, and, at the highest current levels, very rapid onset of f_0 and many higher mode numbers (mf_0). As the injected current is increased, rf activity appears successively at higher harmonics, without any indication of some particular mode being preferentially excited.

Observation of radiated microwave power at L-band ($m \geqslant 4$) and X-band ($m \geqslant 25$) qualitatively support this picture of successively higher modes appearing, and arising earlier in time as the injected current is increased. This is inferred from the "threshold" behavior of the microwave signals (see Fig. 6).

Increasing Landau damping by introduction of an energy spread of $\Delta E/E = 2\%$ into the beam has been observed to increase the current threshold for onset of any of the above phenomenologically-defined effects. Fig. 6 shows a striking example of this. Experiments are now in progress with walls of different surface con-

ductivities, situated at various distances from the median plane, and with inflector structures modified in ways that should influence the collective fields produced by the beam.

As the results reported in the present paper indicate, collective instabilities can be of great importance in an electron-ring device and must be thoroughly mastered if successful operation is to be reliably achieved. Although the performance of Compressor 2 indicated that good performance is obtainable, the design of the interior of that device was sufficiently elaborate as to obscure the influence of the various individual components on the self-fields of the beam. To achieve a more explicit understanding and mastery of collective phenomena, therefore, we are continuing the present systematic experimental study with Compressor 4 and are developing additional computational tools intended to provide a more realistic description of the collective fields that will arise with the configurations that we can investigate.

Acknowledgements

References

1. E.J. Lofgren, "The Berkeley ERA Program", Particle Accelerator Conf., March, 1971.

2. D. Keefe, et al, "Experiments on Forming, Compressing and Extracting Electron Rings for the Collective Acceleration of Ions", UCRL-20144, 1970. Nucl. Instr. and Methods (to be published).

3. W.W. Chupp, et al, "The ERA 4 MeV Injector", Particle Accelerator Conf., March 1971, UCRL-20174.

4. D. Keefe, et al, Phys. Rev. Letters 22, 558, (1969).

5. NUERA is a CDC 6600 computer program developed by L.J. Laslett and B.S. Levine with the help of V.O. Brady and R. Healy. It basically solves the electrical problem for the coupled pulsed electrical circuits of the Compressor and then determines the single-particle equilibrium orbit, vs. time, for an electron in the resulting magnetic field.

6. A.M. Sessler, Lawrence Radiation Laboratory, private communication.

7. L.J. Laslett, Arithmetic Pertaining to Landau Damping for Compressor 4, Lawrence Radiation Laboratory report ERAN-121, Dec. 1970, unpublished.
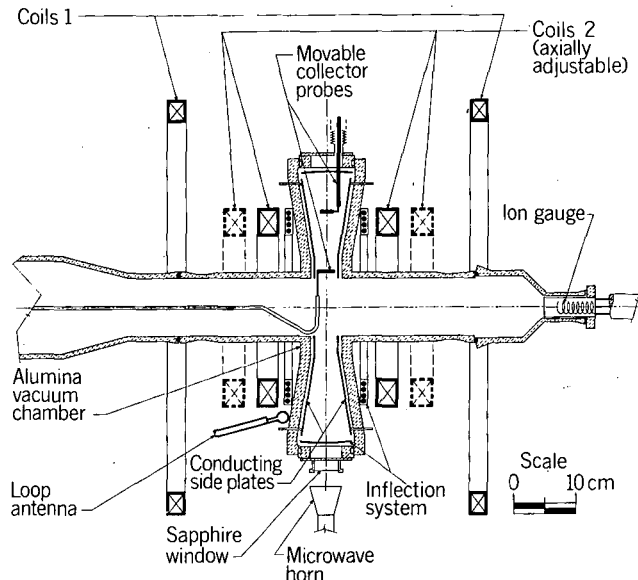
ERA COMPRESSOR 4

XBL 712 6249

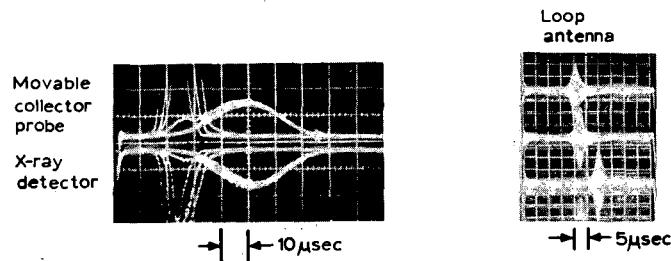Fig. 1 - Cross-section view of Compressor 4.

Fig. 2 - Oscillograms showing both normal spill on probe or early spill due to radial coherent growth. Also shown is accompanying burst of rf at frequency $(1 - \nu_R) f_0$.
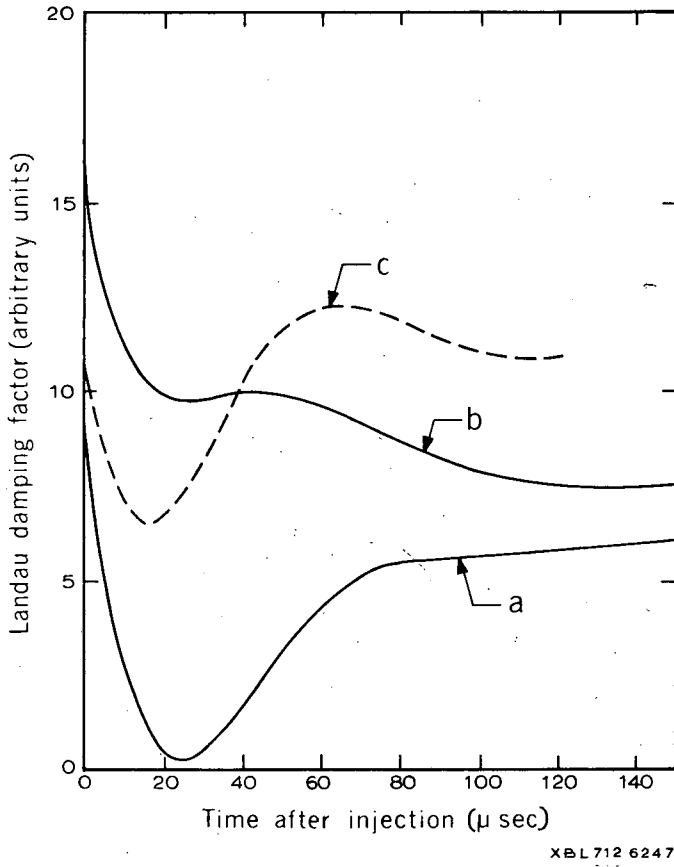
Fig. 3 - Coefficient of ΔE in the Landau damping term versus time after injection for:
(a) Compressor 4 with eddy currents in Coil Set 2;
(b) Compressor 4 without eddy currents in Coil Set 2;
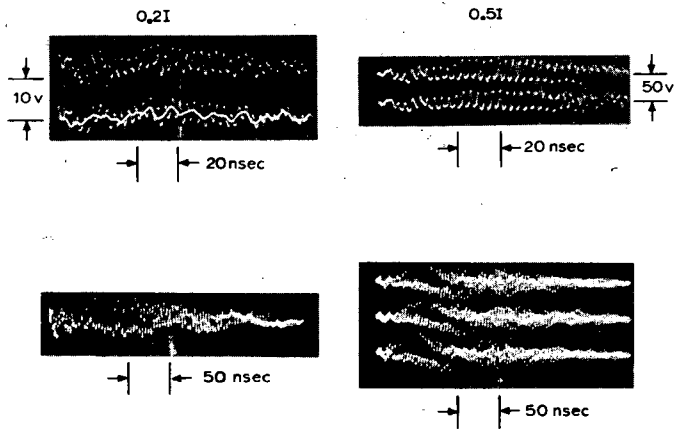(c) Compressor 2 with eddy currents in Coil Set 2 and Coil Set 3 present.
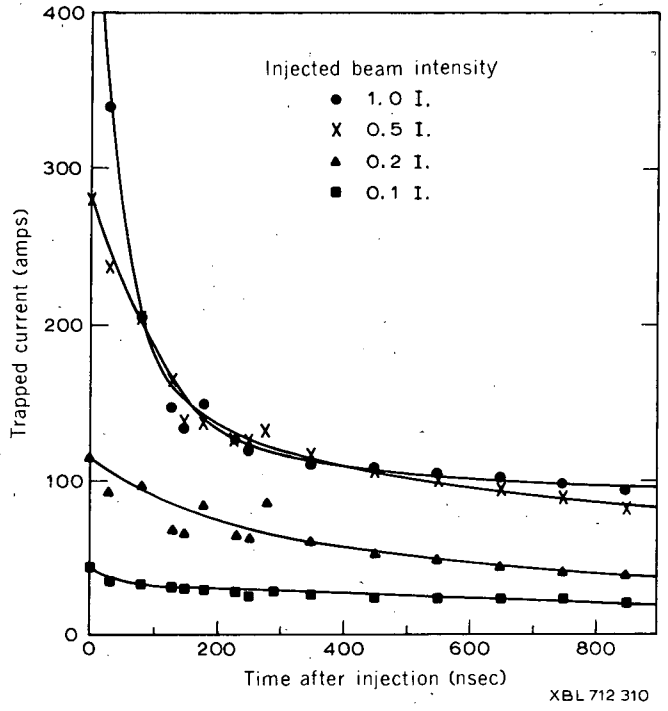

Fig. 4 - Integrated signal from magnetic pick-up loop showing the circulating current during the first 200 turns for various injected beam levels with I_0 designating the unattenuated beam level. The energy spread of the injected beam was 2% (FWHM).

Fig. 5 - Signals from a high frequency pick-up loop close to the beam. The energy spread of the injected beam was 2% (FWHM).
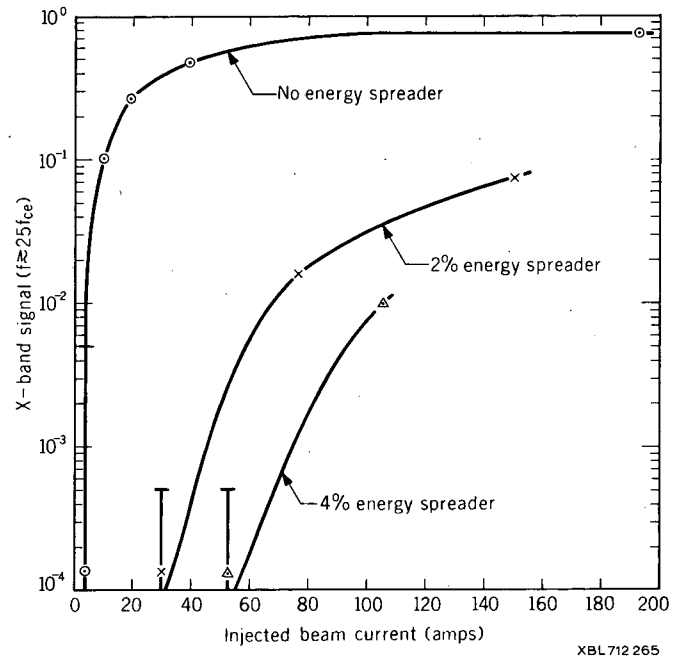
Fig. 6 - Microwave signals (X-band) as a function of the injected beam current (≈ trapped beam current) for (a) no energy spreader, (b) ΔE/E = 2% (FWHM), (c) ΔE/E = 4% (FWHM).

4